

# Remnants of Initial Anisotropic High Energy Density Domains in Nucleus-Nucleus Collisions

F. Wang<sup>a</sup> and H. Sorge<sup>b</sup>

(a) Nuclear Science Division, LBNL, Berkeley, CA 94720, USA

(b) Department of Physics, SUNY at Stony Brook, NY 11794, USA

## Abstract

Anisotropic high energy density domains may be formed at early stages of ultrarelativistic heavy ion collisions, e.g. due to phase transition dynamics or non-equilibrium phenomena like (mini-)jets. Here we investigate hadronic observables resulting from an initially created anisotropic high energy density domain. Based on our studies using a transport model we find that the initial anisotropies are reflected in the freeze-out multiplicity distribution of both pions and kaons due to secondary hadronic rescattering. The anisotropy appears to be stronger for particles at high transverse momenta. The overall kaon multiplicity increases with large fluctuations of local energy densities, while no change has been found in the pion multiplicity.

Under normal conditions, quarks and gluons are confined in hadrons. The situation is entirely different at high densities as may have been created in the early universe shortly after the Big Bang or in today's laboratory experiments in which two nuclei are colliding. It is impossible under such conditions that spatially separated hadrons be formed. Instead, formation of quark matter is expected [1–5]. The primary goal of high energy heavy ion experiments is to create this new state of matter, the quark-gluon-plasma (QGP) in which quarks and gluons are no longer confined in individual hadrons. It is conceivable that a deconfined matter may be formed at an early stage of a heavy ion collision only in a localized region in configuration space, surrounded by hadronic matter. For example, Gyulassy *et al.* [6] argued that as a result of multiple mini-jet production at RHIC energy, the initial conditions of the QGP formed in ultrarelativistic nuclear collisions might be inhomogeneous, with large fluctuations of the local energy density. They showed that such initial conditions could result in azimuthal asymmetry in particle distributions. In contrast to mini-jet production, S. Mrówczyński [7] argued that color filamentation could also result in azimuthal asymmetry by a flow of large number of particles with relatively small transverse momenta. Kapusta *et al.* [8] argued that the probability of a hard nucleon-nucleon collision that was able to nucleate a seed of QGP in the surrounding hot and dense hadronic matter in a central heavy ion collision may not be small even at AGS energy. In addition, disoriented chiral condensates (DCC) may be formed in heavy ion collisions by the restoration of chiral symmetry [9,10]. The formation of DCC could result in a spectacular asymmetry in charged (and neutral) pion phase-space distributions [11].

Once created at early stage of a heavy ion collision, a QGP will undergo a phase transition from the deconfined state to a normal hadronic state, followed by hadronic expansion. What are measured in experiments are the particle momenta long after these particles have ceased to interact (freeze-out). It remains an experimental and theoretical challenge to extract information on the initial conditions from the particle distributions at freeze-out. Early investigation by Pratt [12] showed that two particle correlations may be useful to search for these fluctuations in initial conditions.

Because of secondary particle interactions (hadronic rescattering), primordial quark-gluon distributions from a QGP may be completely altered during the hadronic expansion stage. On the other hand, an initial anisotropy from the quark-gluon stage in configuration space may not be washed out but survive the hadronic stages. Non-isotropic energy densities may leave their imprint on momentum spectra due to hadronic rescattering. Different amounts of rescattering can result in variations of particle multiplicities along different directions. An interesting consequence may be that a non-spherical high energy density domain, which can be formed at an early stage of a heavy ion collision due to fluctuations in energy deposition, may produce an anisotropy in pion and kaon emission after freeze-out. It is the goal of the present work to study the possible magnitude of such an anisotropy, given the magnitude of the initial anisotropy in configuration space.

Since we are going to study the translation of initial spatial anisotropies into final-state momentum anisotropies of kaons and pions due to hadronic rescattering, it is important that the model to be used contains the relevant dynamics and describes existing experimental data to a reasonable degree. One of the important physics results learned from current heavy ion experiments at the BNL AGS and the CERN SPS is that there is a large amount of secondary particle interactions in central collisions. Transport models [13–18] have been employed to

study the importance of these interactions for observables. For example, strangeness yields may change drastically due to the hadronic cascading [19–21]. In fact, the systematics of the observed strangeness enhancement [22–25] – energy and mass dependence – can be described by the Relativistic Quantum Molecular Dynamics (RQMD) approach [26–28] rather well. In this paper, we use the RQMD approach to investigate the translation of initial spatial anisotropies into final-state momentum anisotropies of kaons and pions. One should note, however, that the excess of strange anti-baryons which has been observed [24,29,30] cannot be solely produced by hadronic collisions within the RQMD approach [31]. More complicated mechanisms pointing to earlier and denser stages are required. For instance, formation of color ropes [20,31,32] which has been implemented in RQMD, density-dependent antibaryon masses [33] or quark coalescence [34,35] may be responsible. While the strange antibaryons may well be a very interesting probe of the matter deposition at early times in heavy ion collisions, it should be noted that they are very rare particles at presently accessible energies [36]. Lack of statistics has prevented us to employ these species in the context discussed here of dynamically caused event-by-event fluctuations.

RQMD (version 2.3) [15] was used to simulate head-on Pb+Pb collisions (impact parameter  $b = 0$ ) at SPS energy (158 GeV/nucleon). The influence of the hadronic rescattering on the inclusive yields has already been studied by one of the authors. By including rescattering in RQMD, pion multiplicity is reduced by 8% and kaon multiplicity increases by over 50% at SPS energy [15].

For the present work we did not attempt to include dynamical fluctuations in the local energy deposition other than given by the standard RQMD procedure. Instead, the initial conditions after hadronization as resulting from the model were modified to create artificially anisotropic domains beyond the model’s intrinsic – dynamical and statistical – fluctuations. We feel this is justified in view of the considerable uncertainties in the early-state dynamics which cannot be reliably calculated based on quantum chromodynamics (QCD).

In the following we specify our strategy to include additional fluctuations on an event-by-event basis: At  $t = 1$  fm/c in the center of mass frame, a randomly chosen fraction of hadrons with rapidity  $|y| < 1.5$  was moved into an elliptical area in the transverse plane, located around the center of the fireball, and the longitudinal position ( $z$ ) was kept unchanged. The new  $(x, y)$  positions in the cylinder were randomly sampled from a homogeneous distribution. Size of the transverse cross-section of the cylinder was chosen as 8 fm (major axis)  $\times$  2 fm (minor axis). The total energy and momentum are conserved by this procedure. On the other side, the artificially induced fluctuations of the local hadron densities modify the subsequent collision dynamics. After the re-arrangement, RQMD is properly re-initialized and propagates the hadrons until freeze-out.

We have studied two cases:

1. 10% of the hadrons ( $|y| < 1.5$ ) were moved. Approximately 90 hadrons representing a total energy of 120 GeV were moved in each event. This resulted in a 30% increase of total energy within the cylinder, and a 20–30% increase in the total number of binary collisions. About 11K events were studied for this case.
2. 20% of the hadrons ( $|y| < 1.5$ ) were moved. Approximately 180 hadrons representing a total energy of 240 GeV were moved in each event. This resulted in an 60% increase of total energy within the cylinder, and a 40–50% increase in the total number of binary

collisions. About 10K events were studied for this case.

The left panel of Fig. 1 shows the projection of the particle density onto the  $z = 0$  plane, resulting from the re-arrangement at  $t = 1$  fm in the center of mass frame. The right panel of Fig. 1 shows the level of asymmetry in configuration space due to the creation of a high energy density domain. Fig. 2 shows average energy density within the elliptical cylinder as a function of time in the center of mass frame for the second case. The solid curves are for energy summed over all particles/strings, and the dashed ones are those for particles/strings within  $|y| < 1.5$ . Artificial creation of the high energy density domain is visible as the discontinuity at  $t = 1$  fm. The bases are the time profile of the average energy density from a default RQMD event. Although the energy density in the central elliptical cylinder is artificially increased at the initial stage, the freeze-out density is similar to that from a default RQMD event, as shown in the figure. This indicates that the freeze-out density is constant in RQMD over a wide range of initial conditions.

As discussed at the beginning, the purpose of the study is to investigate possible signatures of high energy density domains at initial stages of heavy ion collisions in the azimuthal distributions of particles at freeze-out. The resulting freeze-out charged pion distribution is displayed in Fig. 3, for the first case in the upper panel and for the second case in the bottom panel. As clearly seen from the figure, the distributions are azimuthally asymmetric. There are fewer pions emitted along the major axis of the ellipse, in agreement with the picture that pion yield is reduced by rescattering [15]. It should be noted that this result qualitatively agrees with the result that the elliptic flow is in-plane at SPS energy for medium impact parameters [37] where the initial geometry is similar to the high energy density domain studied here. Only particles with rapidities  $|y| < 2$  are plotted in the figure. No anisotropy was found for particles with rapidity of more than 2 units away from mid-rapidity. This is presumably due to that only particles within  $|y| < 1.5$  were modified.

The azimuthal multiplicity distributions can be described by the functional form

$$\frac{dN}{d\phi} = 1 - \alpha \cos(2\phi). \quad (1)$$

A fit to the distribution yields  $\alpha = 0.35\%$  and  $0.69\%$  for case 1 and case 2, respectively. The magnitude of the anisotropy,  $\alpha$ , depends upon pion transverse momentum,  $p_\perp$  (GeV/c); the higher  $p_\perp$ , the greater the anisotropy. The azimuthal distributions for pions of different  $p_\perp$  ranges are shown in Fig. 4 for the second case. The fit results of the anisotropy in pion multiplicity distribution for various  $p_\perp$  cuts, as well as the one including all  $p_\perp$  in Fig 3, are summarized in Table I. There is no difference observed between  $\pi^+$  and  $\pi^-$ . The  $p_\perp$  dependence can be qualitatively understood. High  $p_\perp$  pions colliding with other particles have high probability to be destroyed to produce other particles, for instance,  $\pi\pi \rightarrow KK$ . Low  $p_\perp$  pions, on the other hand, more often elastically scatter from other particles resulting in no change of the pion multiplicity. The anisotropy must asymptotically approach zero for zero  $p_\perp$  particles as required from symmetry considerations.

The azimuthal distribution of charged pion multiplicity ( $|y| < 2$ ) from default RQMD events is constant as expected. The fitted average of the distribution from the default events is shown as the dotted line on the plots in Fig. 3 and Fig. 4. There is no essential change in the overall charged pion multiplicity due to the initial high energy density domain. See Table II where the relative changes are tabulated.

The azimuthal distributions of  $K^+$  (left panel) and  $K^-$  (right panel) multiplicities are shown in Fig. 5 for the second case. A cut of  $|y| < 2$  is also applied in all plots. The top two plots are the distributions for kaons including all  $p_\perp$ , whereas the other plots have various  $p_\perp$  cuts. As can be seen from the plots, the kaon multiplicity is anisotropic as well. The fits to the functional form (1) are superimposed on the figure as the solid curves. The fit results of the anisotropy are tabulated in Table I. The magnitude of the anisotropy in the kaon multiplicity is similar to the pions. This indicates that absorption of pions and kaons is similar in the fireball.

However, compared to the kaon multiplicity from the default RQMD events, the overall kaon multiplicity is increased. The fitted average to the kaon multiplicity ( $|y| < 2$ ) from default RQMD events is shown as the straight line on each plot in Fig. 5. The relative increase in  $K^-$  is larger than in  $K^+$ , whereas the absolute increase is similar. For reference, the magnitudes of the absolute and relative increases in kaon multiplicity are tabulated in Tables II and III, respectively. To demonstrate this point more clearly, the azimuthal distributions of the difference in  $K^+$  and  $K^-$  multiplicities are computed and plotted in the top panel of Fig. 6. The solid curves are fits to the functional form (1), and the dotted lines are the fitted average to the corresponding distributions from default RQMD events. As can be seen from the plots, the increase in this quantity from default RQMD events is minor. Presumably, the slight increase in this quantity from default RQMD events is due to the excess in  $K^+$  production (over  $K^-$ ) through associate production together with  $\Lambda$ 's. To illustrate this point, azimuthal distributions of  $\Lambda$  multiplicity are plotted in the bottom panel of Fig. 6. The distributions of  $N_{K^+} - N_{K^-}$  and  $\Lambda$  are indeed similar.

The following picture emerges from the above results. More pions are absorbed along the major axis of the elliptical high energy density domain. Kaons are absorbed in the same manner as pions. The increase in number of binary collisions, presumably, enhances particle production including both pions and kaons. Large fraction of these pions, however, are destroyed by rescattering producing additional kaons. These kaons are produced dominantly through pair production mechanism. There are slight excess in  $K^+$  over  $K^-$  from associate production of  $K^+$  together with  $\Lambda$ 's, mainly in the high  $p_\perp$  region.

In summary, we have quantitatively studied, in the framework of RQMD model, the remnants of non-spherical, high energy density domains in particle emissions at freeze-out. Such domains can produce anisotropy in charged pion and kaon emission at freeze-out due to particle rescattering; the anisotropy persists more in high  $p_\perp$  particles. For a 27% asymmetry in the initial configuration distribution (for the second case), a 0.7% anisotropy was found in the pion distribution at freeze-out. This anisotropy increased from 0.4% for pions with  $p_\perp < 0.5$  GeV/c to 2.2% for pions with  $p_\perp > 0.8$  GeV/c. The factor how the initial asymmetry in configuration space translates into final momentum space appears to be rather small. Depending on the transverse momentum window it varies between 1.5 and 8 percent. The anisotropy shows similar strength in kaon distributions. The addition of the high energy density domain resulted in enhanced kaon multiplicity at freeze-out, while there was essentially no change in the overall pion multiplicity. The increase in kaon multiplicity is mainly due to increased pair production.

The current study used RQMD events simulated with exact zero impact parameter to avoid possible anisotropy in the freeze-out particle multiplicity distribution arising from finite impact parameter. The magnitude of such anisotropy in central collisions at small

finite impact parameters has not been studied in details. The current study assumed that the high energy density domain was present in every event at the center and had the same size and shape. It remains a future task to study the dependence of the anisotropy as functions of location, size and shape of the high energy density domain. In the present work, the anisotropy in particle emission is studied only inclusively. It remains a challenge to study the effect on an event-by-event basis, given the relative weakness of the effect as shown by the present work.

One of the authors (FW) thanks Dr. P. Jacobs, Dr. A. M. Poskanzer, Dr. H. G. Ritter and Dr. N. Xu for valuable discussions. He also thanks the Institute for Nuclear Theory where part of this work was carried out. This work was supported by the U. S. Department of Energy under contracts DE-AC03-76SF00098 and DE-FG02-88ER40388. This research used resources of the National Energy Research Scientific Computing Center.

## REFERENCES

- [1] T. D. Lee and G. C. Wick, *Phys. Rev.* **D9**, 2291 (1974).
- [2] B. D. Keister and L. S. Kisslinger, *Phys. Lett.* **B64**, 117 (1976).
- [3] J. Rafelski, *Phys. Rep.* **88**, 331–347 (1982).
- [4] L. McLerran, *Rev. Mod. Phys.* **58**, 1021–1064 (1986).
- [5] B. Müller, *Nucl. Phys.* **A544**, 95c–108c (1992).
- [6] M. Gyulassy, D. H. Rischke, and B. Zhang, *Nucl. Phys.* **A613**, 397–434 (1997).
- [7] S. Mrówczyński, *Phys. Lett.* **B393**, 26–30 (1997).
- [8] J. I. Kapusta and A. P. Vischer, *Phys. Rev.* **C52**, 2725–2732 (1995).
- [9] K. Rajagopal and F. Wilczek, *Nucl. Phys.* **B399**, 395–425 (1993).
- [10] K. Rajagopal and F. Wilczek, *Nucl. Phys.* **B404**, 577–589 (1993).
- [11] S. Gavin, A. Gocksch, and R. D. Pisarski, *Phys. Rev. Lett.* **72**, 2143 (1994).
- [12] S. Pratt, *Phys. Rev.* **C49**, 2722–2728 (1994).
- [13] H. Sorge, H. Stöcker, and W. Greiner, *Nucl. Phys.* **A498**, 567c–576c (1989).
- [14] H. Sorge, H. Stocker, and W. Greiner, *Annals of Physics* **192**, 266–306 (1989).
- [15] H. Sorge, *Phys. Rev.* **C52**, 3291–3314 (1995).
- [16] L. A. Winckelmann, *Nucl. Phys.* **A610**, 116c (1996).
- [17] Y. Pang, T. J. Schlagel, and S. H. Kahana, *Phys. Rev. Lett.* **68**, 2743–2746 (1992).
- [18] Bao-An Li and Che Ming Ko, *Phys. Rev.* **C52**, 2037–2063 (1995).
- [19] R. Mattiello *et al.*, *Phys. Rev. Lett.* **63**, 1459 (1989).
- [20] H. Sorge *et al.*, *Phys. Lett.* **B289**, 6–11 (1992).
- [21] M. Berenguer, H. Sorge, and W. Greiner, *Phys. Lett.* **B332**, 15 (1994).
- [22] T. Abbott *et al.* (E802 Collaboration), *Phys. Rev. Lett.* **64**, 847 (1990).
- [23] T. Abbott *et al.* (E802 Collaboration), *Phys. Lett.* **B291**, 341–346 (1992).
- [24] J. Bartke *et al.* (NA35 Collaboration), *Z. Phys.* **C48**, 191–200 (1990).
- [25] C. Bormann *et al.* (NA49 Collaboration), *J. Phys.* **G23**, 1817–1825 (1997).
- [26] H. Sorge *et al.*, *Phys. Lett.* **B271**, 37–42 (1991).
- [27] H. Sorge, *Z. Phys.* **C67**, 479 (1995).
- [28] H. van Hecke, H. Sorge, and N. Xu, *Phys. Rev. Lett.* (1998). In press.
- [29] R. Stock *et al.* (NA35 Collaboration), *Nucl. Phys.* **A525**, 221c (1991).
- [30] S. Abatzis *et al.* (WA85 Collaboration), *Phys. Lett.* **B270**, 123 (1991).
- [31] H. Sorge, *Nucl. Phys.* **A566**, 633c (1994).
- [32] H. Sorge, *Nucl. Phys.* **A590**, 571c (1995).
- [33] C. M. Ko, M. Asakawa, and P. Levai, *Phys. Rev.* **C46**, 1072–1076 (1992).
- [34] P. Csizmadia *et al.*, (1998). hep-ph/9809456.
- [35] J. Zimanyi, T. S. Biro, and P. Levai, *J. Phys.* **G23**, 1941 (1997).
- [36] Strangeness, charm and anti-baryon production as probes for QGP formation in nuclear collisions, P. Koch and U. Heinz, In *Proceedings of International Workshop on Quark Gluon Plasma Signatures*, Strasbourg, France, October 1990.
- [37] H. Appelshauser *et al.* (NA49 Collaboration), *Phys. Rev. Lett.* **80**, 4136–4140 (1998).

### TABLES

TABLE I. Pion and kaon emission anisotropy at freeze-out,  $\alpha$ , resulting from the initial anisotropic high energy density domain in central Pb+Pb collisions (impact parameter  $b = 0$  fm) at 158 GeV/nucleon simulated by RQMD.

	particle	all $p_\perp$	$p_\perp < 0.5$	$p_\perp > 0.5$	$p_\perp > 0.8$
case 1	$\pi$	0.3%	0.2%	0.5%	1.0%
	$K^+$	0.3%	0.0%	0.4%	0.7%
	$K^-$	0.4%	0.0%	0.8%	0.7%
case 2	$\pi$	0.7%	0.4%	1.1%	2.2%
	$K^+$	1.1%	0.6%	1.2%	1.9%
	$K^-$	1.0%	0.3%	1.3%	2.0%

TABLE II. Relative increase in pion and kaon multiplicity due to the initial anisotropic high energy density domain from default RQMD events.

	particle	all $p_\perp$	$p_\perp < 0.5$	$p_\perp > 0.5$	$p_\perp > 0.8$
case 1	$\pi$	-0.3%	-0.3%	-0.1%	-0.1%
	$K^+$	4.7%	3.4%	4.7%	8.0%
	$K^-$	6.7%	3.9%	8.2%	11%
case 2	$\pi$	-0.7%	-1.2%	0.2%	1.9%
	$K^+$	3.8%	1.8%	4.0%	9.0%
	$K^-$	5.4%	1.6%	6.8%	12%

TABLE III. Absolute increase in kaon multiplicity due to the initial anisotropic high energy density domain from default RQMD events.

	particle	all $p_\perp$	$p_\perp < 0.5$	$p_\perp > 0.5$	$p_\perp > 0.8$
case 1	$K^+$	0.87	0.32	0.25	0.30
	$K^-$	0.68	0.19	0.24	0.25
case 2	$K^+$	0.72	0.17	0.21	0.34
	$K^-$	0.55	0.08	0.20	0.27

## FIGURES

FIG. 1. RQMD simulation of central Pb+Pb collisions (impact parameter  $b = 0$  fm) at 158 GeV/nucleon: a high density domain is created at an initial stage ( $t = 1$  fm in the center of mass frame) by moving 10% (case 1) or 20% (case 2) hadrons into an elliptical cylinder at the center of the fireball. Particle density at  $t = 1$  fm projected on the  $z = 0$  plane is shown at the left. The high energy density domain is shown in the sketched ellipse. Anisotropy in configuration space is shown at right for the two initial conditions studied.

FIG. 2. Average energy density in the cylinder (in a typical event) as a function of time in the center of mass frame. The solid curves are energy density calculated from all particles. The dashed curves are energy density calculated from particles with rapidity  $|y| < 1.5$ . The lower solid curve and the lower dashed curve are the corresponding energy density from a default RQMD event. The increase in the energy density at  $t = 1$  fm corresponds to creation of the high energy density domain (case 2).

FIG. 3. Azimuthal distribution of charged pion multiplicity at freeze-out for case 1 (top) and case 2 (bottom). Only pions with rapidity  $|y| < 2$  are included.  $\phi = 0$  corresponds to the major axis ( $+x$  in Fig. 1) of the ellipse of the high energy density domain. The solid curve is a fit to the functional form (1). The dotted line is the average charged pion multiplicity in default RQMD events.

FIG. 4. Azimuthal distribution of charged pion multiplicity at freeze-out in rapidity  $|y| < 2$  for various  $p_{\perp}$  cuts for case 2.

FIG. 5. Azimuthal distribution of  $K^+$  (left) and  $K^-$  (right) multiplicity at freeze-out in rapidity  $|y| < 2$  for various  $p_{\perp}$  cuts for case 2.

FIG. 6. Azimuthal distribution of the difference between  $K^+$  and  $K^-$  multiplicities (top) and  $\Lambda$  multiplicity (bottom) at freeze-out in rapidity  $|y| < 2$  for case 2.

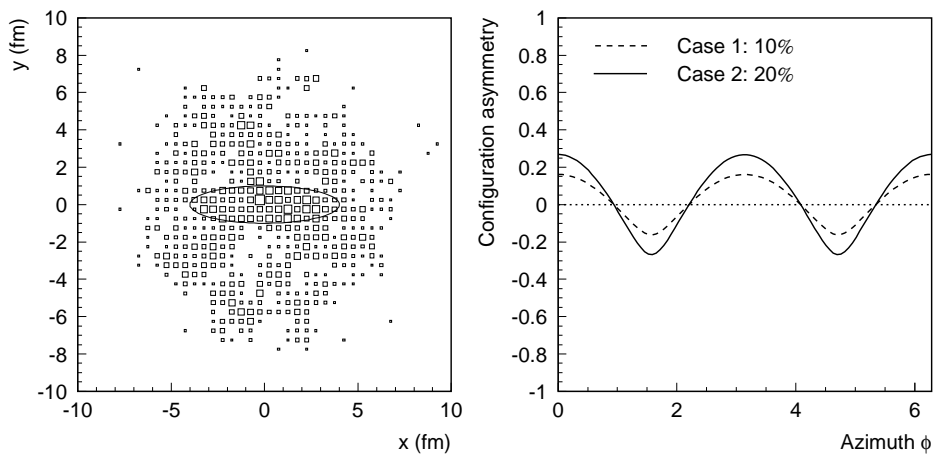


Figure 1

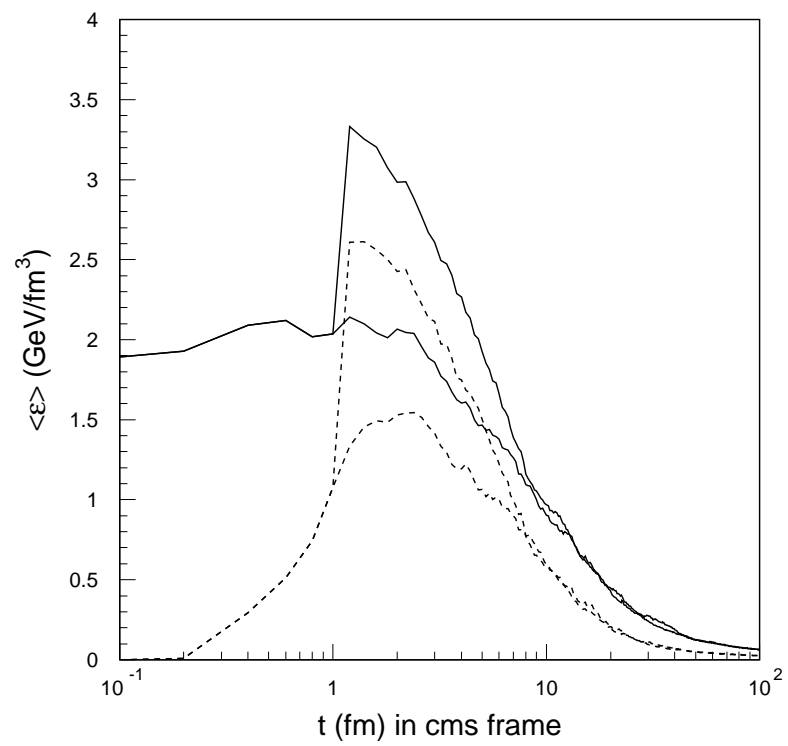


Figure 2

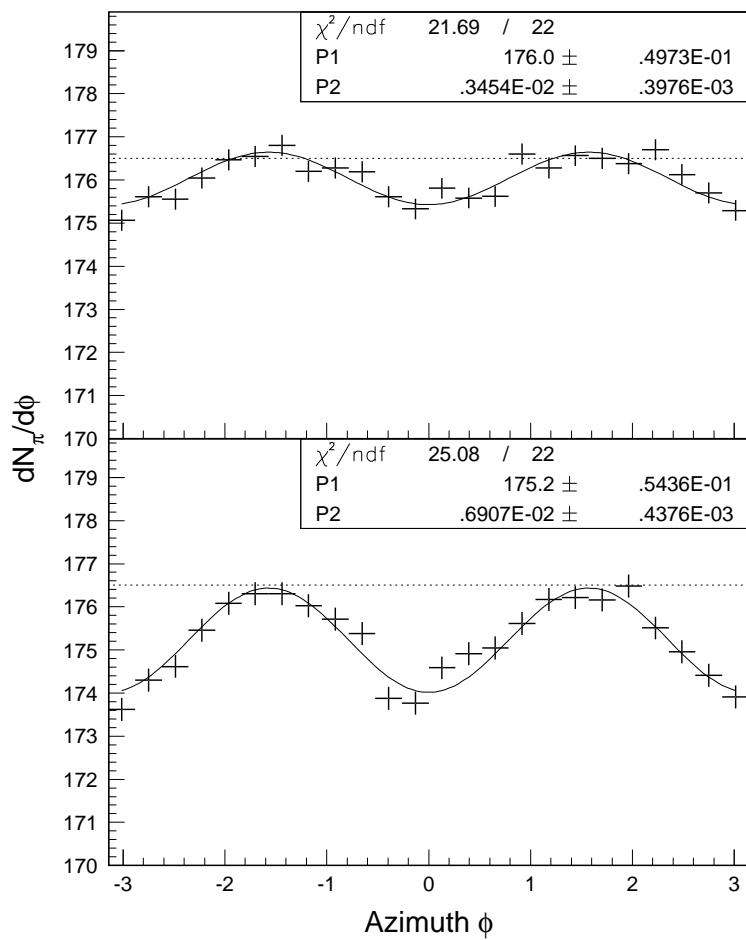


Figure 3

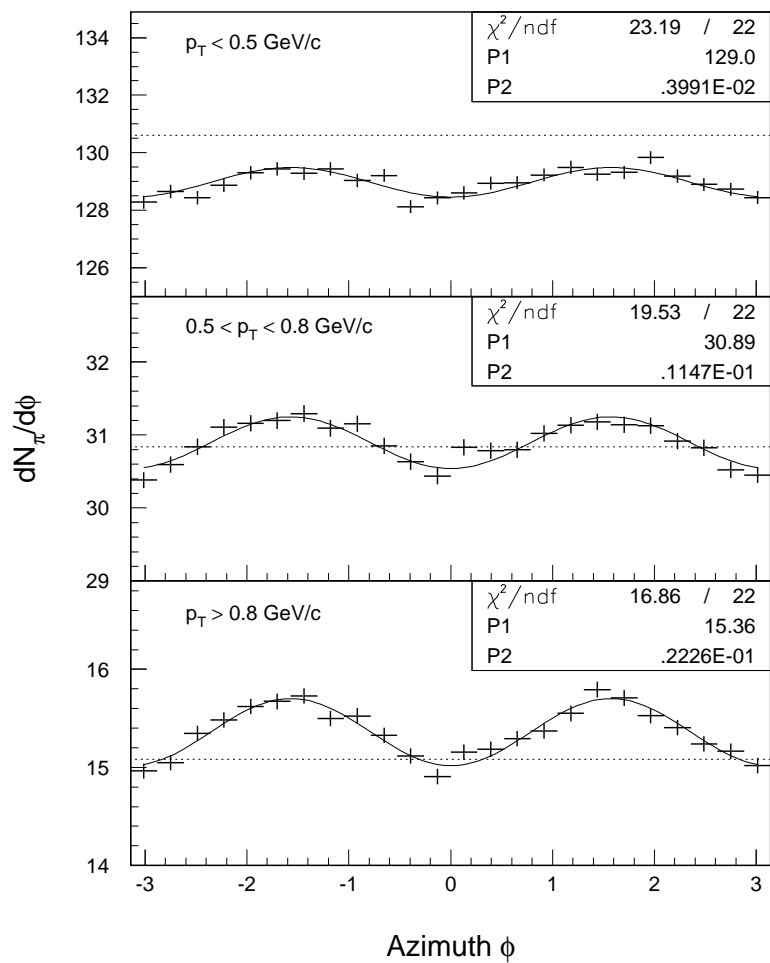


Figure 4

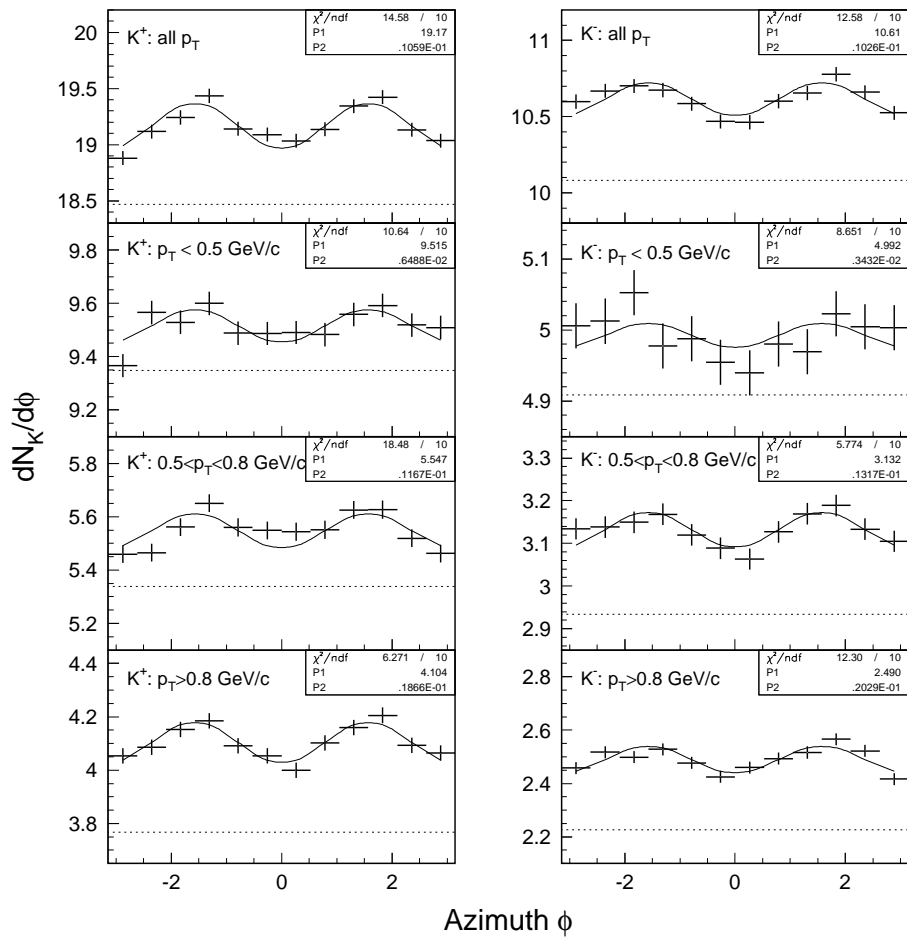


Figure 5

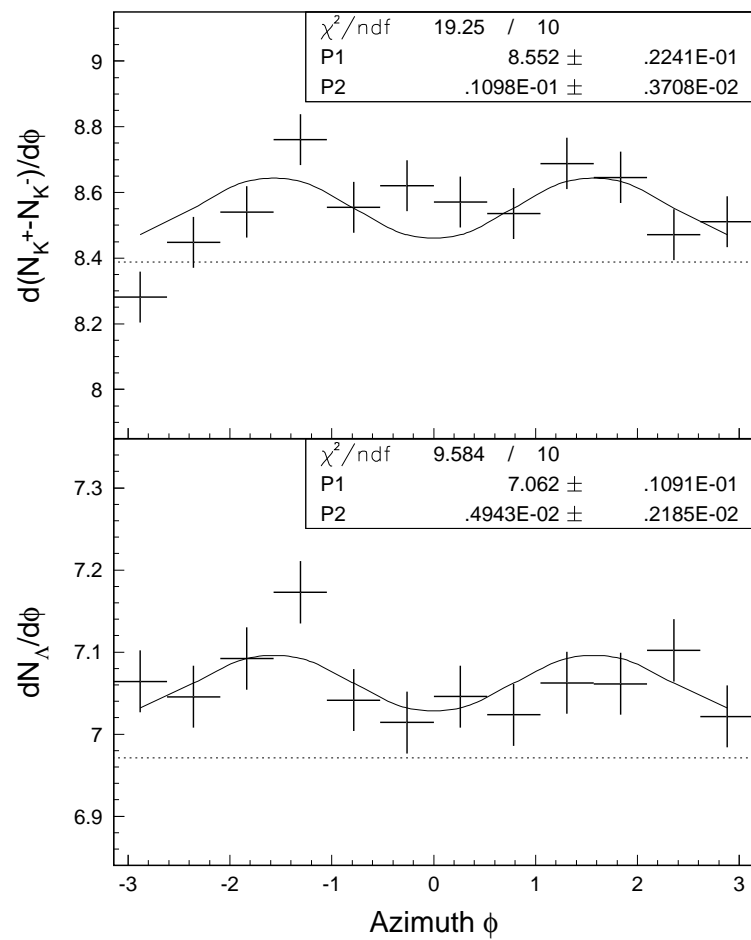


Figure 6